6th European Conference on Computational Mechanics (ECCM 6)
7th European Conference on Computational Fluid Dynamics (ECFD 7)
11-15 June 2018, Glasgow, UK

RELIABILITY-BASED DESIGN OPTIMIZATION OF A SUPERSONIC NOZZLE

RICHARD W. FENRICH, VICTORIEN MENIER, PHILIP AVERY, AND JUAN J. ALONSO

Stanford University
450 Escondido Mall, Stanford, USA
e-mail: rfenrich@stanford.edu

Key words: Optimization, Reliability, Multifidelity, UQ, CFD, FEA

Abstract. The practical application of reliability-based design optimization (RBDO) requires both accurate models and efficient reliability analysis and optimization methods. However, these methods become prohibitively expensive for complex multiphysics engineering applications. In addition, the robust implementation of such multiphysics packages is nontrivial. As a result, we have developed a a new multifidelity RBDO approach and a multiphysics simulation suite for supersonic nozzles to demonstrate the application of RBDO to a complex coupled aerospace design problem. Our results illustrate the use of a reliability-based design workflow, the challenges of developing a robust multiphysics model, and show the benefits of using design under uncertainty methods for the design of a reliable supersonic nozzle.

1 INTRODUCTION

Complex multidisciplinary design problems are common in engineering and often rely on simplified models with little multiphysics coupling. In addition, uncertainty in the operating environment and the system itself is often only roughly and usually conservatively characterized using a safety factor despite being an influential factor for design. Thus both integrating higher-fidelity coupled multiphysics models into the design process and more accurately quantifying the uncertainty in a design's performance can help improve a system's reliability from the beginning of the design process and avoid costly fixes later in the design process or even after manufacturing.

In this paper we discuss the application of reliability-based design optimization (RBDO) to the design of a supersonic nozzle. The supersonic nozzle design problem was selected due to its inherent multiphysics nature requiring aerodynamic, thermal, and structural analyses, as well as the ample presence of uncertainties ranging from material properties to inlet and atmospheric conditions [1]. Figure 1 shows the different components modeled in the non-axisymmetric nozzle system. We consider a critical top-of-climb design condition where temperatures and stresses are the highest. 40 random variables were identified and characterized from experimental data, simulations, or expert judgment. Our goal

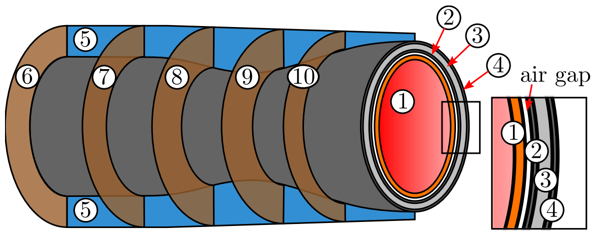

Figure 1: Schematic of nozzle components.

Number	Component Name
1	thermal layer
2	inner load layer
3	middle load layer
4	outer load layer
5	stringers
6-10	baffles 1-5

Table 1: Component numbering.

is twofold: 1) to introduce an RBDO approach and show its benefits over traditional deterministic design, and 2) to describe the construction and challenges associated with developing a coupled multiphysics model for design under uncertainty.

Section 2 introduces RBDO, the nozzle optimization problem, and elements of the RBDO process including dimension reduction, a multifidelity optimization approach, and uncertainty quantification. Section 3 explores the construction and challenges associated with building and validating a suite of multifidelity aero-thermal-structural models for the nozzle design problem. Section 4 shows the optimal reliable nozzle design and compares it to an optimal deterministic nozzle design. Finally, section 5 concludes with lessons learned and future directions for the design of reliable complex engineering applications.

2 RELIABILITY-BASED DESIGN OPTIMIZATION

A reliability-based design optimization (RBDO) problem can be written formally as a stochastic optimization problem over deterministic variables x and random variables ξ, where one or more of the objectives or constraints seek a small probability of failure, *i.e.* a reliable design. A typical form of the RBDO problem is shown in equation 1:

$$\begin{aligned} \underset{x,\xi}{\text{minimize}} \quad & E[f_0(x,\xi)] \\ \text{s.t.} \quad & P\left[f_i(x,\xi) \leq 0\right] \leq p_{f,i} \quad i = 1 \ldots m \end{aligned} \tag{1}$$

where $f_i(x,\xi)$ are the stochastic quantities of interest in the problem, and $p_{f,i}$ is the allowable probability of failure associated with chance constraint i, typically calculated through a reliability analysis. Often the chance constraints are rewritten using an inverse formulation known as the performance measure approach such as $F_i^{-1}(p_{f,i}) \geq 0$ where F_i^{-1} is the inverse CDF for $f_i(x,\xi)$ [2]. Such a formulation avoids issues during the optimization when the calculated probability of failure is zero.

The problem in equation 1 is difficult for general nonlinear f_i due to the need to evaluate quantities of interest multiple times in reliability analyses and over the course of the optimization. Many methods have been proposed for solving or approximating a solution to RBDO problems including double-loop methods, sequential methods, and unilevel methods [2], the latter two of which have shown promise in decreasing the cost of obtaining a solution. In addition, the use of surrogate models and/or multifidelity techniques can be used to additionally decrease cost when function evaluations are expensive [3]. Lastly, in addition to efficient optimization and reliability analysis methods, dimension

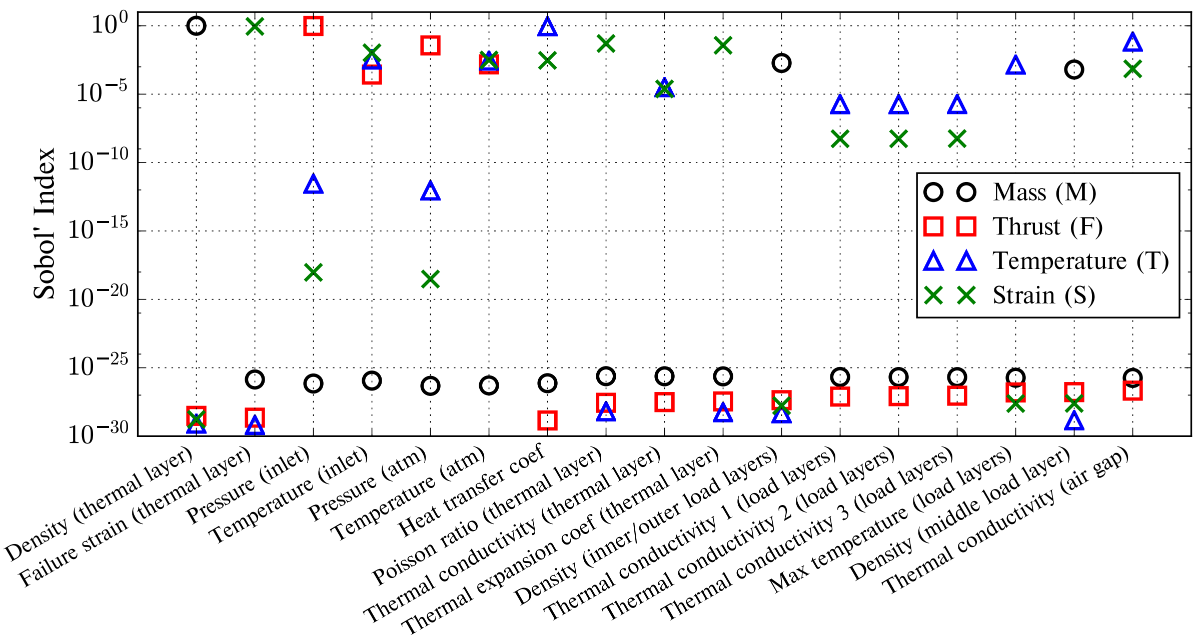

Figure 2: Total-order Sobol' indices for the 17 random variables which contribute most to the variance of the four quantities of interest considered in the nozzle problem. Eliminating variables with indices less than 10^{-5} reduces the problem's random dimension from 40 to 14. First-order Sobol' indices (not shown) are nearly the same implying interaction effects can be neglected.

reduction is also a critical technique for the successful application and solution of large-scale RBDO problems. In many applications, only a subset or specific combinations of the design variables x or random parameters ξ contribute to variations in the quantities of interest, allowing a reduction in problem size and therefore expense to be made.

In this paper we consider the RBDO problem for a supersonic nozzle shown in equation 2. We consider 54 deterministic design variables and 14 random parameters. The quantities of interest include the mass of the nozzle M, the thrust of the nozzle F, a temperature failure criterion in the inner load layer T, and a strain failure criterion in the thermal layer S. Mass is selected as a surrogate for cost in the aerospace design problem and the constraints were selected from a larger set of 15 on various nozzle components after random sampling and deterministic optimization showed thrust, thermal failure in the load layer, and structural failure in the thermal layer to be the most critical quantities.

$$
\begin{aligned}
\underset{x \in \Re^{54}}{\text{minimize}} \quad & E[M(x,\xi)] & \\
\text{s.t.} \quad & P\left[F(x,\xi) \leq 21500\right] & \leq 10 \times 10^{-4} \\
& P\left[T(x,\xi) \geq 1\right] & \leq 10 \times 10^{-4} \\
& P\left[S(x,\xi) \geq 1\right] & \leq 10 \times 10^{-4} \\
& Ax \leq b &
\end{aligned}
\tag{2}
$$

2.1 Dimension reduction via Sobol' indices

Global sensitivity measures such as Sobol' indices can be used to justify dimension reduction. Since Sobol' sensitivity indices measure the variation in a function $f(\xi)$ due to each input ξ_i, variables which contribute little to variation in $f(\xi)$ can be fixed at nominal values with little to no loss of response fidelity. For dimension reduction, one should consider the total-order Sobol' index which estimates the total effect of ξ_i on $f(\xi)$.

Sobol' indices can be motivated by first recalling the definition for total variance of a function: $\mathrm{Var}(f(\xi)) = D(\xi) = \int f^2(\xi)d\xi - (\int f(\xi)d\xi)^2$. Then, the total variance can be decomposed as:

$$D(\xi_1, \ldots, \xi_n) = \sum_{i=1}^{n} D_i(\xi_i) + \sum_{1 \le i \le j \le n} D_{ij}(\xi_i, \xi_j) + \ldots + D_{1,\ldots,n} \tag{3}$$

Details and an interpretation in light of Analysis of Variance (ANOVA) can be found in Archer et al [4]. Sobol indices are defined as:

$$S_{i_1,\ldots,i_s} = \frac{D_{i_1,\ldots,i_s}}{D} \tag{4}$$

The total-order Sobol' index for ξ_i is calculated by summing all Sobol' indices which incorporate a contribution from ξ_i. Figure 2 shows the total-order Sobol' indices calculated for the 4 quantities of interest considered in the nozzle design problem.

2.2 Trust region model management of multifidelity surrogates

When $f_i(x, \xi)$ is expensive to evaluate, a surrogate model or lower-fidelity physics-based model can be used as a proxy for truth function evaluations during optimization. However, such models also usually exhibit reduced accuracy over a portion of the design space and require periodic corrections or adaptive updates. Trust region model management is a technique for managing such a collection of multifidelity models during optimization [3]. The key idea is to solve a series of cheaper optimization subproblems within a trust region using a less accurate lower-fidelity model that is periodically corrected with high-fidelity model information. The trust region location and size is updated after each subproblem and represents the user's confidence in the accuracy of the lower-fidelity model.

There are many guidelines for constructing a successful trust region model management optimization algorithm and Eldred and Dunlavy provide a concise overview of the working components [3]. For provable convergence to a local minimum, the low-fidelity model must be corrected to match both the function values and gradients of the high-fidelity model at the trust region center at the start of each subproblem. The accuracy and correlation of the low-fidelity model, as well as the selection of the initial trust region size can have a large impact on the efficiency of the algorithm. Lastly, several varieties of trust region update and acceptance logic have been proposed in the literature in an attempt to speed up convergence and avoid infeasible subproblems. In this paper we use a filter method for trust region acceptance, an adaptive penalty merit function, and what Eldred and Dunlavy refer to as a direct surrogate trust region formulation. In addition we use a sequential method for solving the RBDO problem; as a result the reliability analysis used to obtain constraint values is only performed once per subproblem in the trust region model management algorithm. See Fenrich and Alonso for details [1].

2.3 Reliability analysis with polynomial chaos

Solving RBDO problems for complex applications rests largely on the ability to accurately identify the limit state $f_i(x, \xi) = 0$ and efficiently estimate a probability of failure p_f or a response level $f(x, \xi)$ corresponding to a given probability of failure:

$$p_f = P[f(x, \xi) \leq 0] = \int_{f(x,\xi)\leq 0} p(\xi) d\xi \tag{5}$$

Sampling methods for estimating p_f from equation 5 such as direct Monte Carlo, importance sampling, or directional simulation typically require too many function evaluations to be efficient when expensive multiphysics simulations are used [5, 6]. Other common methods include the First Order (FORM) and Second Order (SORM) Reliability Methods which grew out of the structural reliability community and can be efficient and accurate for limit states which are close to linear [6]. Nonlinear limit states can be addressed with response surface methods where the limit state is approximated by a polynomial, Gaussian process regression model, or other response surface and then p_f is estimated more cheaply from the response surface. However, care must be taken to ensure the response surface is very accurate in regions contributing greatly to p_f [5].

In this paper we consider a response surface method where the limit state is approximated with orthogonal polynomials through a method known as generalized polynomial chaos [7]. In other words we approximate $f(\xi)$ as:

$$f(\xi) \approx \sum_{i=1}^{Q} a_i \Psi_i(\xi) \tag{6}$$

where the polynomial expansion has been truncated to include Q terms involving coefficients a_i and basis functions $\Psi_i(\xi)$. The benefits of the generalized polynomial chaos expansion include an analytical estimate of the mean and variance of $f(\xi)$ in terms of the coefficients a_i and adaptivity and error estimates for the approximation. Details can be found in Xiu and Karniadakis [7] regarding optimal bases and calculation of coefficients a_i. Once the expansion is constructed, Monte Carlo sampling can be used to estimate p_f.

3 MODEL DEVELOPMENT

We have developed an automated suite of coupled multidisciplinary analysis tools for the static aero-thermal-structural analysis of supersonic nozzles called MULTI-F. MULTI-F is written in Python and calls the open source codes SU2 [8] and AERO-S [9] for fluid and thermal/structural analyses, respectively. It features a hierarchy of model fidelity levels, ranging in both the physical fidelity (Quasi-1D/Euler/RANS for fluids and linear/nonlinear for structures) and mesh discretization. Users can easily run coupled aero-thermal-structural analyses for user-specified nozzle geometries, material combinations,

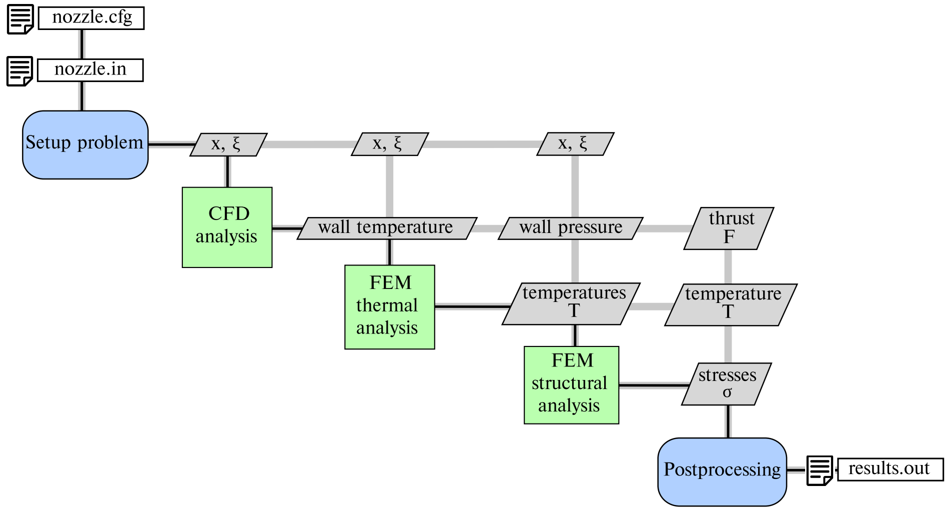

Figure 3: Workflow and capabilities of multifidelity aero-thermal-structural analysis suite MULTI-F. The user provides a configuration file specifying the problem and a corresponding input file specifying design variable values. MULTI-F then performs the required analyses and outputs results to a file.

and environmental parameters by managing a configuration file and associated input file specifying variable values. Figure 3 shows the workflow and capabilities of MULTI-F.

3.1 Shape parameterization

The chosen parameterization for the nozzle's inner wall consists of a circular inlet that is blended to an elliptical exit with a flattened bottom edge. Each nozzle cross section is defined using an ellipse and the entire nozzle shape is parameterized with three B-splines: one for the centerline and two for the major and minor axes of the elliptical cross sections, see Figure 4. A corresponding 2D axisymmetric geometry for lower-fidelity models is constructed by taking equivalent area cross-sections. Wall layer thicknesses are parameterized using piecewise bilinear functions. A series of linear constraints for the shape parameterization variables was also developed to ensure reasonable nozzle geometries during sampling and optimization.

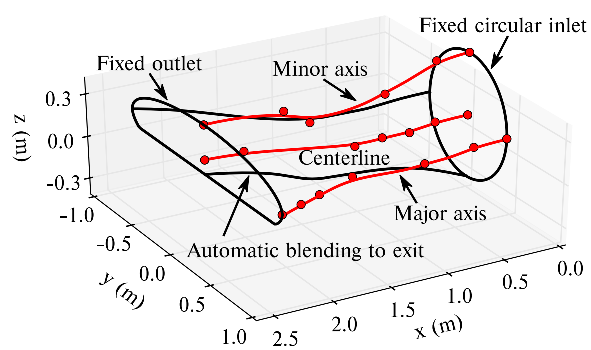

Figure 4: 3D nozzle inner wall shape parameterization showing B-splines and control points. A set of linear constraints ensures control points are well spaced and steep changes in geometry are avoided.

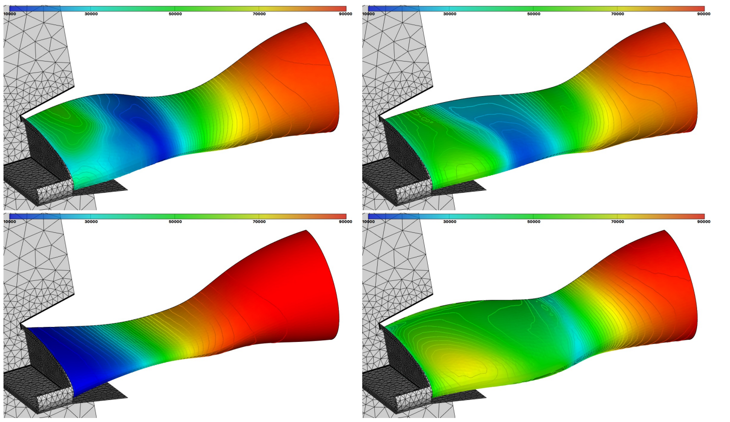

Figure 5: Randomly sampled 3D nozzle shapes are used to assess general robustness of the aerodynamic model. Here pressure contours from 3D RANS solutions are shown.

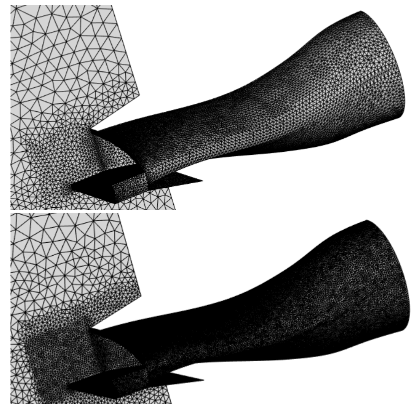

Figure 6: Coarse (top) and fine (bottom) Euler meshes.

3.2 Aerodynamic model

The internal and external nozzle flow is calculated using SU2, an open-source software suite for multiphysics simulations [8]. The steady, compressible Euler or RANS equations are solved in 2D or 3D, depending on the specified model fidelity. Since even small changes in the nozzle shape can have a dramatic impact on the flow physics, particularly near the throat of the nozzle, the aerodynamic model must be robust in addition to accurate and reasonably fast. As a result, the quality of the baseline meshes as well as the flow solver parameters had to be carefully tuned. A quasi-1D area-averaged Navier Stokes aerodynamic model with conjugate heat transfer modeled using thermal resistances was also developed to serve as a low-fidelity model.

For the higher-fidelity models, the governing Euler or RANS equations are discretized in SU2 using a finite volume method with a standard edge-based data structure. The control volumes are constructed using a median-dual, vertex-based scheme. The convective fluxes are discretized using the second-order accurate JST scheme [10] and the Menter SST turbulence model [11] is employed for viscous simulations. The time integration is performed using an Euler implicit method and the linear system is solved using the Generalized Minimal Residual (GMRES) method. In order to damp low-frequency errors an agglomeration multigrid method is employed.

For each fidelity level, a sequence of three increasingly refined baseline meshes was crafted ranging from coarse to fine as shown in figure 6. First, an initial mesh is generated using Gmsh [12] with different levels of refinement for the nozzle interior, exit, plume, mid-field and far-field regions. Next, the mesh is remeshed using the Feflo.a-AMG Inria library [13] to satisfy mesh size requirements. For RANS meshes a quasi-structured boundary layer mesh is also generated using Bloom, a viscous mesh generator developed at Inria [14]. During optimization, these baseline meshes are deformed to fit the nozzle geometry by analytically projecting the baseline mesh onto the new geometry and then running the SU2 mesh deformation module to ensure good quality of the volume mesh.

3.3 Thermal and structural models

The nozzle thermal and structural analyses are calculated using AERO-S, an open-source finite element method (FEM) analysis software [9]. An elastostatic boundary value problem representing the equilibrium of internal and external forces is considered for the structural analysis while a Poisson boundary value problem representing the steady state heat transfer is considered for the thermal analysis. One-way coupling is assumed between the analyses: the temperature obtained from the aerodynamic analysis furnishes the boundary condition on the inner wall of the thermal model, and the pressure and temperatures obtained from the aerodynamic and thermal analyses respectively furnish the inner wall pressure and the temperature distribution used in the structural analysis. The other boundary conditions are state-independent; a convection boundary condition is specified on the outer wall of the thermal model, while a fixed displacement boundary condition is imposed on the outer edges of the baffles and stringers in the structural model.

The fidelity of each of the structural and thermal models is specified by defining the mesh resolution and degree of geometric approximation. We consider three mesh resolutions and an axisymmetric and nonaxisymmetric nozzle geometry (see figure 7). In the case of the structural model only, the fidelity can be specified further by selecting between a linear analysis in which small displacements are assumed and a nonlinear analysis in which no such assumption is made. For the thermal analysis conventional 8-node hexahedral finite elements and a linear analysis were used. The geometries and meshes were generated using the OpenCascade library and the transfinite meshing algorithm of the Gmsh library [12].

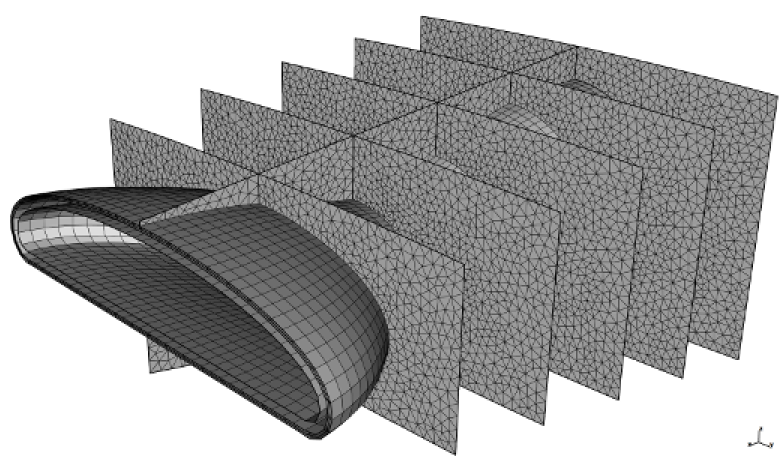

Figure 7: Structural model with geometry specified using the three-dimensional parameterization.

A multi-layer elastic shell is used to model the different layers in the nozzle wall (components 1-4 in figure 1) and accounts for thermal strains which are the major contribution to total strain in the nozzle structure. The deformation of such a layered shell is modeled using standard Kirchhoff thin-plate kinematics; the mid-surface in-plane strains and curvatures are assumed constant and integration through the thickness is performed in a piece-wise manner using constant constitutive properties for each layer. We use layered composite finite elements with three nodes and six degrees of freedom per node [15] each constructed by superposing a membrane triangle with drilling degrees of freedom [16] and an assumed natural deviatoric strain (ANDES) bending triangle [17]. Lastly, to account for large displacements and associated geometric nonlinearity in the high-fidelity model, the co-rotational formulation is used [18]. This projection-based technique filters out the potentially large rigid body component of each element's motion, leaving only a relatively small elastic deformation to which the theory of linear elasticity can be applied.

3.4 Model validation

In addition to classical code-to-code comparisons of the aero-thermal-structural nozzle model, an assessment of smoothness of the model's quantities of interest should be performed since numerical noise can adversely impact gradient-based optimization algorithms. To this end suites of random parameter sweeps in both the deterministic design variables and random parameters were conducted as aids to identify numerical noise issues due to lack of convergence or other software bugs.

4 RESULTS

We compare reliable nozzle designs from the solution of the reliability-based design optimization (RBDO) problem stated in equation 2 (reformulated using the performance measure approach) with designs from the solution of an equivalent deterministic nozzle optimization where random variables have been fixed at their mean values. The reliable nozzle designs are obtained from the multifidelity optimization approach using trust region model management discussed in this paper and found in more detail in Fenrich and Alonso [1]. The deterministic optimizations are inherently single-fidelity and require no such approach. The high-fidelity model is taken to be a 3D nonaxisymmetric Euler aerodynamic analysis coupled with the 3D nonaxisymmetric linear thermal and structural FEM models. The low-fidelity model is taken to be a quasi-1D area-averaged aerodynamic analysis coupled with 2D axisymmetric linear thermal and structural FEM models. Stochastic quantities are estimated via Monte Carlo sampling ($N = 10^6$) from the polynomial chaos expansions (sparse grid level 1) for each quantity of interest.

Table 2 summarizes the optimization results and figure 8 compares each nozzle's optimal inner wall geometries. Sequential quadratic programming is used to solve each optimization with finite difference gradients. Step sizes and convergence tolerances are estimated from the parameter sweeps used to assess model noise.

As shown in table 2, the deterministic optimizations obtain a much lower expected mass due to the lack of chance constraints on thrust, temperature, and stress and are also correspondingly less reliable. However, when we perform RBDO with the approach outlined in this paper, we are able to achieve a much more reliable nozzle with a reasonable increase in computational cost and of course, an increased mass objective. We emphasize the benefits of performing dimension reduction via Sobol' indices as a first step in the RBDO process which allowed us to reduce the potential cost of the optimization problem

Optimization	Fidelity	Evaluations	$E[M(x,\xi)]$	$p_{f,F}$	$p_{f,T}$	$p_{f,S}$
Deterministic	Low	16	274.55	5.20×10^{-1}	6.39×10^{-1}	0
RBDO	Low	153	517.27	9.50×10^{-5}	0	0
Deterministic	High	4	277.39	9.31×10^{-3}	0	0
RBDO (MF)	High	147	349.29	9.80×10^{-5}	0	0

Table 2: Comparison of optimization results. The reliability of deterministic designs is obtained via a post-processing step where a polynomial chaos expansion is constructed and sampled to obtain failure probabilities. The high-fidelity RBDO uses the multifidelity (MF) method outlined in this paper. Function evaluation counts during the optimization do not include finite differences. The additional cost of solving the RBDO problem is primarily due to the required reliability analyses.

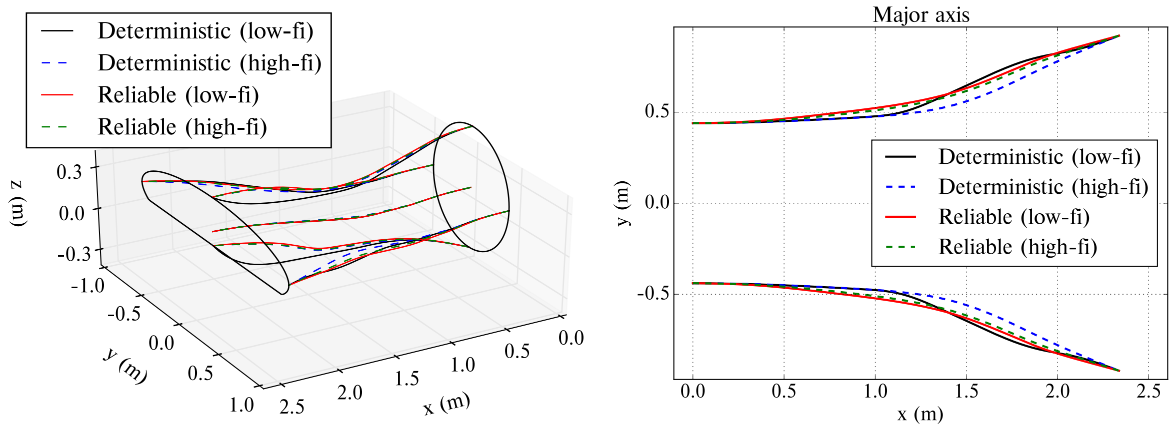

(a) Optimal inner wall geometries

(b) Optimal major axis

Figure 8: Comparison of optimal inner wall geometry with a close-up of optimal major axis geometry for the low-fidelity and high-fidelity deterministic and stochastic optimizations. Differences in centerline geometries for all nozzles are barely discernable, however minor differences in optimal minor axis geometry exist, with the exception of the deterministic low-fidelity optimal result. Note that a throat is present in the nozzle designs due to the flattening out of the elliptical cross-sections.

by approximately 3 times. In addition, the solution of the RBDO problem has given us valuable information on which quantities of interest are the most critical for reliability; in this case thrust is the driving constraint. This is reflected in the shape of the reliable nozzle designs which feature a larger throat area primarily due to a wider major axis which leads to increased mass flow rate and therefore increased thrust. We additionally note that the primary cost of the optimizations is in the evaluation of finite difference gradients, followed by the reliability analyses for the stochastic optimizations.

5 CONCLUSIONS

In this paper we have reviewed the development of a coupled aero-thermal-structural supersonic nozzle model called MULTI-F and its use in deterministic and reliability-based design optimization (RBDO) problems. We affirm that the use of complex engineering models in reliable design poses significant challenges that require careful validation and development effort to ensure robust and accurate model analyses. A well-posed parameterization and associated constraints, and parameter sweep studies are instrumental in achieving successful optimization results. In addition, we note that designing a complex reliable system can be approximated and made tractable through the use of multifidelity methods and selection of efficient uncertainty quantification methods, leading to more reliable performance than traditional design methods for a reasonable increase in computational cost. However, RBDO is still very expensive for large-scale multidisciplinary problems and we emphasize the need for high performance computing and further development of efficient and accurate reliability methods. Analytic sensitivities, when available, can also be immensely helpful in further decreasing cost. Finally, full coupling between a model's disciplines can further increase model fidelity. The authors plan on investigating adaptive sampling and response surface methodologies for more accurate estimation of tail probabilities, and the application of the above optimization framework to the higher-fidelity models included in MULTI-F such as 3D RANS.

Acknowledgements The authors would like to acknowledge the support of the DARPA Enabling Quantification of Uncertainty in Physical Systems (EQUiPS) program and Paul Constantine and Jeffrey Hokanson for their help in assessing model robustness.

REFERENCES

[1] Fenrich, R.W. and Alonso, J.J. Reliable multidisciplinary design of a supersonic nozzle using multifidelity surrogates. *18th AIAA/ISSMO Multidisciplinary Analysis and Optimization Conference*. Denver, Colorado, 2017.

[2] Agarwal, Harish. Reliability based design optimization: formulations and methodologies. PhD Dissertation. University of Notre Dame, 2004.

[3] Eldred, M.S. and Dunlavy, D.M. Formulations for surrogate-based optimization with data fit, multifidelity, and reduced-order models. *11th AIAA/ISSMO Multidisciplinary Analysis and Optimization Conference*. Portsmouth, Virginia 2006.

[4] Archer, G.E.B., Saltelli, A. and Sobol, I.M. Sensitivity measures, ANOVA-like techniques, and the use of bootstrap. *Journal of Statistical Computation and Simulation*. (1997) **58(2)**:99-120.

[5] Li, J., Li, J. and Xiu, D. An efficient surrogate-based method for computing rare failure probability. *Journal of Computational Physics*. (2011) **230(24)**:8683-8697.

[6] Ditlevsen, O. and Madsen, H.O. *Structural Reliability Methods*. Wiley, 2nd Edition, 2005.

[7] Xiu, D. and Karniadakis, G. Modeling uncertainty in flow simulations via generalized polynomial chaos. *Journal of Computational Physics*. (2003) **187(1)**:137-167.

[8] Economon, T.D., Palacios, F., Copeland, S.R., Lukaczyk, T.W., and Alonso, J.J. SU2: An Open-Source Suite for Multiphysics Simulation and Design. *AIAA Journal.* (2015) **54(3)**:828-846.

[9] Farhat, C. AERO-S: A general-purpose finite element structural analyzer. `https://bitbucket.org/frg/aero-s`. 2018.

[10] Jameson, A., Schmidt, W., and Turkel, E.L.I. Numerical solution of the Euler equations by finite volume methods using Runge Kutta time stepping schemes. *14th Fluid and Plasma Dynamics Conference*, Fluid Dynamics and Co-located Conferences, Palo Alto, California, 1981.

[11] Menter, F.R. Two-equation eddy-viscosity turbulence models for engineering applications. *AIAA Journal.* (1994) **32(8)**:1598-1605.

[12] Geuzaine, C. and Remacle, J.F. Gmsh: A 3D finite element mesh generator with built-in pre-and post-processing facilities. *International Journal for Numerical Methods in Engineering.* (2009) **79(11)**:1309-1331.

[13] Loseille, A. and Menier, V., Serial and Parallel Mesh Modification Through a Unique Cavity-Based Primitive BT. *Proceedings of the 22nd International Meshing Roundtable.* Springer International Publishing, Cham, 2014, pp. 541-558.

[14] Alauzet, F. and Marcum, D. A Closed Advancing-Layer Method with Changing Topology Mesh Movement for Viscous Mesh Generation BT. *Proceedings of the 22nd International Meshing Roundtable.* Springer International Publishing, Cham, 2014, pp. 241-261.

[15] Hemez, F. The 3-node composite shell and isoparametric Timoshenko beam elements. *Report CU-CAS-94-16, Center for Aerospace Structures, University of Colorado.* Boulder, Colorado 1994.

[16] Alvin, K., de la Fuente, H.M., Haugen, B. and Felippa, C.A. Membrane triangles with corner drilling freedoms – I. The EEF element. *Finite Elements in Analysis and Design.* (1992) **12**:163-187.

[17] Militello, C. and Felippa, C.A. The first ANDES elements: 9-dof plate bending triangles. *Computer Methods in Applied Mechanics and Engineering.* (1991) **93(2)**:217-246.

[18] Nour-Omid, B. and Rankin, C.C. Finite rotation analysis and consistent linearization using projectors. *Computer Methods in Applied Mechanics and Engineering.* (1991) **32**:353-384.